

Demonstrating a Refinery-adapted cluster-integrated strategy
to enable full-chain CCUS implementation - REALISE

D2.3 HS-3 campaign at the Irving Oil Whitegate refinery

Eirini Skylogianni (TNO), Andreas Grimstvedt (SINTEF),
Solrun Johanne Vevelstad (SINTEF), Roberta Veronezi
Figueiredo (TNO), Donal McSweeney (Irving Oil Whitegate
refinery), Juliana Monteiro (TNO)

08-12-2022

Document History

Revision History

This document has been through the following revisions:

Version No.	Revision Date	Brief Summary of Changes	Name
1.0	2022-09-28	The draft version of the report for submission. The final version will be prepared and resubmitted when analysis of samples is completed.	Eirini Skylogianni
2.0	2022-11-29	Final version of report for submission.	Eirini Skylogianni

Authorisation

This document requires the following approvals:

AUTHORISATION	Name	Signature	Date
WP Leader	Peter van Os		7-12-2022
Project Coordinator	Inna Kim	Inna Kim	08-12-2022





This project has received funding from the European Union's Horizon 2020 research and innovation programme under grant agreement No 884266

© REALISE Consortium, 2022

This document contains information which is proprietary to the REALISE consortium. No third-party textual or artistic material is included in the publication without the copyright holder's prior consent to further dissemination by other third parties.

Reproduction is authorised provided the source is acknowledged.

Disclaimer

The contents of this publication are the sole responsibility of the author(s) and do not necessarily reflect the opinion of the European Union.



Executive summary

CO₂ capture using HS-3 solvent (aqueous mixture of 40wt% of 1-(2-Hydroxyethyl)pyrrolidine, 1-(2HE)PRLD and 15wt% of 3-amino-1-propanol, 3A1P) has been successfully demonstrated at Irving Oil Whitegate Refinery in Ireland with real flue gas, reaching TRL 6. TNO's miniplant, an ATEX-compliant small-scale pilot plant, has been employed to capture CO₂ from flue gases of four different sources of the Irving Oil Whitegate Refinery. The flue gases have varying content of CO₂, O₂ and other impurities in order to degrade and stress-test as much as possible the stability of the solvent. In order to study the multi-absorber concept for capturing CO₂ from different stacks proposed in REALISE, the same solvent was used during all the demonstration campaigns.

The miniplant was operated at stable conditions for more than 3000 operating hours, providing insights regarding the overall performance of HS-3 solvent, including ease-of-operation, capture capacity, degradation and emissions. It has been found that HS-3 solvent is easy-to-use in a CO₂ capture system, since it is non-toxic and did not precipitate, even during unplanned shut-downs. The solvent seems to show slow mass transfer, however it is noted that the solvent was diluted as the campaigns progressed. Another point of attention is the volatility of one of its containing amines, 1-(2HE)PRLD. The latter leads to significant emissions of this component, despite the use of one water wash, and points towards the requirement of using more than one water washes to control the emission levels.

Concerning analytics, the major degradation components of HS-3 solvent are AP-urea and pyrrolidine. This is in agreement with what has been observed previously in a smaller cycled degradation rig (as reported previously in D1.1) and holds also in the case of diluted solvent composition. With the exception of the last campaign with the fourth flue gas used in this work, the nitrogen balance over the liquid samples was closed, indicating that the major degradation compounds with nitrogen have been accounted for. The results of the metal content analysis, which was done to investigate any corrosion-related issues, show concentrations less than 2 mg/L of Fe and of Cr in the end of the campaign, though up to 20 mg/L for Ni.



Table of Contents

1	Introduction	5
2	Equipment, materials and methods	6
2.1	ATEX-compliant small-scale pilot plant	6
2.2	Solvent and flue gases	8
2.3	Analytical methods	8
2.3.1	Gas phase	8
2.3.2	Liquid phase	8
3	Approach	10
3.1	Selection of stacks	10
3.2	Operational settings	10
4	Results	11
4.1	Flue gas composition	11
4.2	Operating conditions	13
4.3	Stability of HS-3 solvent	17
4.3.1	Degradation trends	17
4.3.2	Metals' concentration and corrosion	21
5	Conclusions and further work	22
6	References	23



1 Introduction

CO₂ capture using the HS-3 solvent was demonstrated at Irving Oil Whitegate Refinery in Ireland, as a first step of the evaluation of the multi-absorber concept for capturing CO₂ from different stacks of a refinery studied within REALISE. The work included the building of an ATEX-compliant small scale capture plant, called miniplant, and the demonstration in a refinery by capturing CO₂ from various stacks and, thus, exposing the HS-3 solvent in different flue gas impurities, typical of refinery flue gases. The solvent was not changed in between the tests with the different flue gases, therefore stress-testing the stability and performance of the solvent. By using the same solvent, impurities from different stacks were accumulated over time, thus mimicking the proposed full-scale strategy in which the rich solvent from each stack is combined into one stream to be sent to a single stripping island.

In this work, the preparation of the campaigns, the selection of the stacks, the operational settings as well as the analytical methods and the results of the demonstration activities are presented. *Section 2* describes the CO₂ capture plant and the methods used for the quantification of results. The approach which was followed in the demonstration activities is explained in *Section 3*, while, in *Section 4*, the results both in terms of operational parameters and analytical measurements are presented. Conclusions and further work are given in the end of the report.

The work presented deviates from the project proposal description regarding the demonstration of countermeasures DORA and IRIS on-site. It was expected that the two technologies would have reached the level of development at which they would require minimum intervention by the operators. However, that was not the case, and their usage requires close follow-up and high attention by the operator. In addition, issues with the company for sample transportation resulted in long delays of samples' receipt and analysis, meaning that the need for the application of countermeasures could not be assessed. These reasons, in combination with the limited time available by the Irving Oil operators, led to the decision not to operate DORA and IRIS on-site, and instead demonstrate these technologies in the lab, to allow for close follow-up by the TNO operators. Degraded HS-3 solvent from the campaign at Tiller pilot plant will be used for these tests.



2 Equipment, materials and methods

2.1 ATEX-compliant small-scale pilot plant

A small-scale mobile pilot plant, called miniplant, has been used for the demonstration activities. The miniplant was designed and built by TNO, having a capacity to process up to 5 Nm³/h gas and producing up to 25 kg CO₂ /day. Various carbon capture-related technologies, such as specific solvents, solvent management and emission mitigation technologies, are brought up to TRL 5 and 6 (Technology Readiness Level) when tested in the miniplant in the lab and on-site, respectively.

In order to operate the miniplant in a refinery, it had to become ATEX-compliant. This means that it complies with the European ATEX (ATmosphères Explosives) regulations, thus ensuring safe operations in environments where gaseous combustible materials may be present. This was done by means of positive pressure in a contained space. Two configurations were assumed; one configuration assumed 2 containers, one in horizontal and one in vertical position, while the second configuration assumed 3 containers stacked in horizontal position. The latter was chosen, a preliminary design of which is shown in *Figure 1*, with main selection criteria being easy of operation, stability, cost and delivery time.

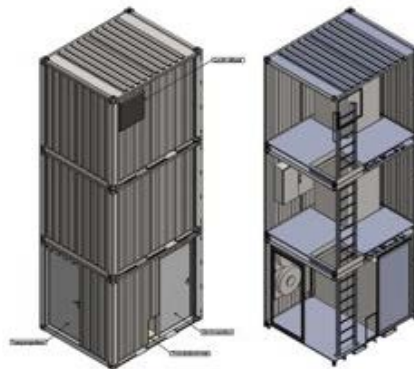


Figure 1. Chosen configurations for ATEX-compliance.

The miniplant is fully automated allowing for continuous operation, whereas during the on-site work, it is operated and controlled remotely by TNO, requiring minimum intervention on-site. A picture of the miniplant is shown in *Figure 2*, when standing and when it is being transported.



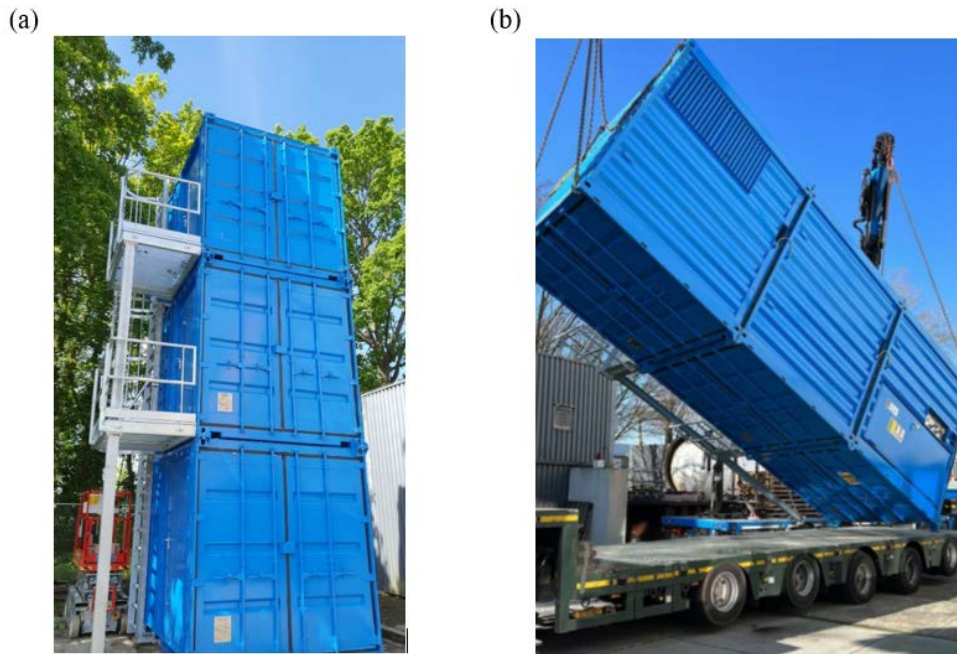


Figure 2. (a) Miniplant standing; (b) Easy transportation of the miniplant.

The main characteristics of the miniplant are shown in Table 1. It is equipped with 4.3 m packing height in the absorber and 1.9 m in the stripper, connected to each other with a cross heat exchanger (HX). Three washes are used: one serves as a direct contact cooler, called a quench, for flue gas conditioning and removal of impurities (i.e. SO_x) and two water washes in both absorber and stripper top for water balance and amine losses control. The solvent inventory is approximately 20L. The flue gas entering the plant is a slipstream of ca. 4 m³/h from the process flue gas.

Table 1. Miniplant’s main characteristics.

Characteristic	Unit	Absorber	Stripper	Water Washes
Packing type	-	Sulzer BX SS	Sulzer BX SS	Sulzer BX SS
Packing height	m	4.25	1.87	1.53
Diameter	m	0.045	0.045	0.045



2.2 Solvent and flue gases

HS-3 is an open novel solvent developed in HiperCap project [1], [2] and optimized within REALISE in order to be used in the demonstration activities. It is an aqueous mixture of 40wt% of 1-(2-Hydroxyethyl)pyrrolidine, 1-(2HE)PRLD, (CAS: 2955-88-6) and 15wt% of 3-amino-1-propanol, 3A1P, (CAS: 156-87-6). The purity of both these non-toxic chemicals was 99 wt%, while demineralized water was used for preparing the solvent.

Real industrial flue gas was used from the Irving Oil Refinery, consisting of mainly nitrogen (N₂), carbon dioxide (CO₂) and oxygen (O₂), and other impurities such as sulfur oxides (SO_x), nitrogen oxides (NO_x) and carbon monoxide (CO). There are 15 sources of flue gas in the refinery, 4 of which were selected to be tested. The stacks from which flue gas was used are hereafter called Stack #1, Stack #2, Stack #3 and Stack #4. The selection details are given in sub-section 3.1.

2.3 Analytical methods

2.3.1 Gas phase

A Fourier-transform infrared spectroscopy (FTIR) analyzer (GasMET CX/DX 4000) was used for the measurement of gas composition. The gas is sampled by means of a heated probe. A short, heated line (180 °C) carries the gas from the sampling probe to the FTIR analyzer. The analyzer has been calibrated for standard inorganic components (NH₃, H₂O, SO₂, NO_x, CO, CO₂) and the HS-3 comprising amines, and is equipped with a ZrO₂ sensor for oxygen measurement.

2.3.2 Liquid phase

Liquid samples (lean and rich) were taken twice a week and sent to SINTEF's MS laboratory for analysis. In this way, the stability of the solvent and potential corrosion in the pilot plant was studied as a function of operation time.

Total Inorganic Carbon-Total Organic Carbon (TIC-TOC) was used for CO₂ loading measurement. Oxidative catalytic combustion and chemiluminescence detection (Shimadzu TOC-L CPH TNM-L) was employed for total nitrogen measurement, while Karl-Fischer (KF) titration was occasionally used for water content quantification. Liquid Chromatography – Mass Spectrometry (LC-MS) was used for the quantification of the concentration of amine/degradation products, as shown in [Table 2](#). As an indication of corrosivity, metal content was also measured employing Inductively Coupled Plasma-Mass Spectrometry (ICP-MS).



Table 2. Degradation compounds analysed using LC-MS in this work.

Name	CAS	Abbreviation
3-(methylamino)-1-propanol	42055-15-2	Methyl-AP
1,3-oxazinan-2-one/tetrahydro-2H-1,3-oxazin-2-one	5259-97-2	OZN
N,N'-bis(3-hydroxypropyl)-urea	71466-11-0	AP-urea
Pyrrolidine	123-75-1	Pyrrolidine
3-methyl-pyridine	108-99-6	3-MPy
N-(3-hydroxypropyl)- β -alanine	55937-35-4	HPAla
N-(3-hydroxypropyl)-glycine	100747-20-4	HPGly
N-(3-hydroxypropyl)-formamide	49807-74-1	HPF
tetrahydro-1-(3-hydroxypropyl)-2(1H)-pyrimidinone	670227-88-0	tHHPP
3-[(3-aminopropyl)amino]-1-propanol	40226-15-1	APAP
Glycolic Acid	79-14-1	Glycolic Acid
3-OH Propionic Acid	503-66-2	3-OH Propionic Acid
Lactic Acid	50-21-5	Lactic Acid
Formic Acid	64-18-6	Formic Acid
Acetic Acid	64-19-7	Acetic Acid
Propionic Acid	79-09-4	Propionic Acid
Isobutyric Acid	79-31-2	Isobutyric Acid
N-Butyric Acid	107-92-6	N-Butyric Acid
Glyoxylic Acid	298-12-4	Glyoxylic Acid
Ammonia	7664-41-7	NH ₃
Methylamine	74-89-5	MA
Ethylamine	75-04-7	EA
Propyl-amine	107-10-8	Propyl-amine
Dimethylamine	124-40-3	DMA
Ethylmethylamine	624-78-2	Ethylmethylamine
Diethanolamine	109-89-7	DiEA
Dipropyl-amine	142-84-7	Dipropyl-amine
Formaldehyde	50-00-0	Formaldehyde
Acetaldehyde	75-07-0	Acetaldehyde
Acetone	67-64-1	Acetone
N-Nitrosodiethanolamine	1116-54-7	NDELA
Nitrosodimethylamine	62-75-9	NDMA
Nitrosodiethylamine	55-18-5	NDEA
Nitrosopiperidine	100-75-4	NPIP
Nitroso N-Methylethylamine	10595-95-6	NMEA
Nitrosopyrrolidine	930-55-2	NPYR



3 Approach

3.1 Selection of stacks

At Irving Oil Whitegate Refinery, there are 15 emission points, 4 of which were selected to capture CO₂ from. The main selection criteria were: their distance between the stack and the miniplant's location inside the refinery, the number of impurities, their CO₂ content and flue gas availability during the period the miniplant was on-site. More information on the emission points and stack selection was given in D2.1. The duration of the campaigns, excluding unplanned shut-downs, is given in [Table 3](#).

Table 3. Duration of demonstration campaigns.

Campaign	Period	Operating Hours per Campaign
Stack #1	13/4 – 23/6	654
Stack #2	23/6 – 2/8	918
Stack #3	2 – 29/8	547
Stack #4	1 – 6/9	90

3.2 Operational settings

Based on prior testing and de-risking activities as well as testing during the commissioning of the miniplant on-site, the main operational settings were decided ([Table 4](#)).

Table 4. Main operating settings.

Operating setting	Unit	Value
Gas inlet flowrate	Nm ³ /h	~4
Liquid flowrate (lean)	kg/h	~12
Liquid inlet temperature	°C	40
Water wash inlet temperature	°C	40
Stripping temperature	°C	120
Stripping pressure	barg	0.95



4 Results

4.1 Flue gas composition

During the commissioning of the miniplant, the FTIR was used to measure the gas composition at both the absorber inlet and the absorber wash outlet. Since changing the measurement point with the FTIR requires human intervention, it was decided to fix it to the outlet of the absorber wash for the duration of the campaign in order to measure emissions to the atmosphere. This meant that for Stacks #2 to #4, when TNO personnel was not on-site, the inlet gas composition was measured by stopping the solvent circulation for adequate time to “saturate” any remaining solvent in the packing of the absorber column, and measuring in the outlet of the water wash. For Stack #1, the flue gas composition was measured both in the start and the end of the campaign, in order to evaluate possible flue gas fluctuation. Particle measurements using the ELPI+ (Electrostatic Precipitator) are typically measured, however, in this work, such measurements were not possible to be conducted, because the operation of the ELPI+ requires the production of a corona charge, which is not ATEX-compliant.

Table 5 presents the results of the flue gas composition measurements. For Stack#1, where measurements were conducted both in the start and the end of the campaign, insights regarding the degree of flue gas composition fluctuation can be extracted. It can be seen that the CO₂ and oxygen content are very similar, while for the rest of the impurities some variation is seen. The largest difference is shown for CO where ~4 and ~90 mg/Nm³ are measured in the start and the end of the campaign, respectively, as well as for NO_x with ~40 and ~20 mg/Nm³, respectively. For Stacks #2 and #3, one measurement was done in the start of the campaign, while for Stack #4 in the end. It is noted that due to water condensing in the non-insulated line during transport from the stack to the miniplant, the water content is expected to be lower than the one out of the stack while specific compounds which are soluble in water, such as NO₂, are not expected to be present in the measured stream.

Table 5. Flue gas composition.

Component	Unit	Stack 1 (start)	Stack 1 (end)	Stack 2	Stack 3	Stack 4
CO ₂	vol%	5.9	5.3	8.2	5.5	6.0
O ₂	vol%	7.8	7.6	4.6	12.9	11.0
H ₂ O	vol%	1.8	2.1	4.3	4.0	3.5
CO	mg/Nm ³	3.9	90.2	0.0	0.0	0.0
N ₂ O	mg/Nm ³	0.0	0.2	0.0	0.0	0.0
NO _x	mg/Nm ³	40.3	23.7	67.4	43.1	61.3
SO ₂	mg/Nm ³	1.1	0.0	0.0	-	-
CH ₄	mg/Nm ³	2.1	3.6	1.9	1.6	1.5

It should be noted that furnace operational data is variable throughout the year because of continuous adjustments made to fuel gas burner efficiency as well as continuous adjustments made to the furnace fuel gas composition. Nevertheless, the following observations can be made:



The measurements of oxygen and CO₂ concentration are compared with the measurements conducted by the refinery the previous year (2021) in Table 6. For the comparison, the concentrations are expressed in dry basis. For Stack #1 where two series of composition measurements are available, the average value is used for the comparison. The rest of the impurities are not included given the already observed variation with time.

Table 6. Comparison of CO₂ and O₂ concentration (dry basis) measured during the campaigns in 2022 and measured by the refinery in 2021.

Component	Unit	Stack 1		Stack 2		Stack 3		Stack 4	
		Irving	TNO	Irving	TNO	Irving	TNO	Irving	TNO
CO ₂	vol%	8.1	5.6	5.5	8.2	6.3	5.5	6.8	6.0
O ₂	vol%	6.0	7.7	10.7	4.6	8.6	12.9*	7.8	11.0*

*measurements disregarded due to sensor

It is seen that, regarding carbon dioxide concentration, the measured concentrations are similar for Stack #3 and Stack #4, with a relative deviation (RD) of 12%. However, for Stack #1 the measured CO₂ content is lower by ~3 vol% (RD=31%) and for Stack #2 it is higher by ~3 vol% as well (RD=49%). These deviations are significant and could be attributed either to FTIR measurement inaccuracy or the already mentioned process variation between the two measurements or fluctuations. After the end of the campaigns, the accuracy of the FTIR was checked against reference gases (CO₂-N₂ mixtures controlled by mass flow controllers) with CO₂ concentration ranging from 5 to 20 vol% (Table 7). The maximum absolute relative deviation (ARD) is 2.4 while the average ARD is 1%. Therefore, it is concluded that the differences seen between the measurements in 2021 and 2022 are attributed to process variations and/or flue gas composition fluctuations.

Table 7. Comparison CO₂ concentration FTIR measurement with reference value.

Reference CO ₂ vol%	FTIR measurement CO ₂ vol%	ARD* %
5.03	4.91	2.4
9.99	9.88	1.1
15.02	14.98	0.3
19.98	20.05	0.4
<i>average</i>		<i>1.0</i>

*Absolute Relative Deviation. $ARD = |CO_{2\text{ FTIR}} - CO_{2\text{ ref}}| / CO_{2\text{ ref}}$

The measured oxygen content is in better agreement between the two measurements for Stack#1, and significantly deviates for Stacks #2 to #4. For Stack #2, the measured O₂ concentration is 4.6 compared to 10.7 by Irving Oil. For Stacks #3 to #4, it is measured by TNO higher by ~4 vol%. In the start of the campaigns, the oxygen sensor was calibrated and when exposed to air during the change from one stack to another, it was further validated. During changes in Stack #3 campaign, it was observed that the O₂ measurement in air was ~23 vol%. This is evidently wrong and the result of a failure of the sensor, thus, these measurements are discarded. Therefore, for the evaluation of degradation results, the O₂ content informed by Irving Oil is assumed. The overestimation of the oxygen content does not apply to the results of Stack #2, since the measurement in 2022 is significantly lower, thus it



can be the result of process variations. It is noted that the oxygen sensor is independent from the FTIR measurement, therefore the erroneous oxygen measurement did not propagate to erroneous FTIR measurements.

4.2 Operating conditions

The operating conditions in the start and in the end of each campaign are given in [Table 8](#). For Stack #4, which only lasted for a few days, the mean value during the campaign is reported.

It is easily noticed that no significant variations are observed in terms of operating settings and temperature profiles during each campaign. An exception to this is the campaign with Stack #3, where towards the end of the campaign, the cross-heat exchanger and absorber temperatures are slightly increased. This is probably the result of higher gas flowrate in the end of the campaign while using the same liquid solvent flowrate. Moreover, during the campaign with Stack #3, malfunction of the lean flowmeter occurred, and as a result the flowrate and thus the levels in the absorber and the stripper were not balanced, leading to instabilities in the plant.

Looking at the temperature profiles in the absorber, the typical bulge temperature (or the maximum temperature recorded) is seen in the top of the absorber. The location of the bulge depends primarily on CO₂ concentration, capture rate, heat of absorption, L/G ratio and absorber height. For full-height absorbers and fast solvents, the temperature bulge appears in the bottom or in the lower part of the column. Having a temperature bulge higher and on the top of the column indicates slow mass transfer while also pointing towards the limited height of the column. This is expected due to the fact that the miniplant is a pilot with limited height, not specifically optimized for HS-3. It should be noticed, however, that while the height of the miniplant is limited, it uses a dense packing, thus offering high contact area between the liquid and the gas. For solvents with higher mass transfer rate, such as 30wt%, when operating around the same conditions (L/G, partial pressure of CO₂), capture rates in excess of 90% are achieved in the miniplant. This observation is also in-line with the measurements reported in D1.1, in which the kinetic constant of HS-3 is ca. 1 order of magnitude lower than that of 30wt% MEA in the temperature range between 40 and 60 °C (see Figure 3-32 of that report).

Regarding the capture rates, there are three different ways to calculate it: based on the CO₂ amount in the CO₂-lean stream leaving the plant from the absorber side (gas side), based on the CO₂ amount in the CO₂ stream leaving the plant from the stripper side (gas side), and based on the analysis of the liquid samples (liquid side). Overall, large deviation is seen between the gas side and the liquid side calculation. The calculation from the liquid side is consistently higher than the rest, and the calculation from absorber side is always higher than when calculated from the stripper side. The capture rate based on the liquid side for Stack #1 is not given since it is calculated to be >100%, which has no physical meaning. Moreover, the capture rates from the stripper side for Stack #3 are not reported since a leakage in the CO₂ exit line was suspected, which was found during the change from Stack #3 to Stack #4.

[Table 8](#). Overview of operational parameters used in the demonstration for each stack.

Parameter	Unit	Stack 1		Stack 2		Stack 3		Stack 4
		Start	End	Start	End	Start	End	Mean
<i>Gas and liquid flows</i>								



Gas inlet	Nm ³ /h	3.97	3.95	3.81	3.70	3.81	4.20	4.01
Liquid inlet	kg/h	12	11.9	12	12.1	11.9	12.3	12.5
L/G absorber	kg/kg	2.3	2.3	2.4	2.5	2.4	2.2	2.4
<i>Temperatures</i>								
Liquid inlet	°C	35.8	37.9	37.2	39.5	39.4	41.1	41.6
Gas inlet to absorber	°C	22.9	24.5	19.3	23.8	22.5	23.1	22.9
Absorber bottom packing	°C	35.7	34.8	35.8	38	33.6	37.1	33.9
Absorber intermediate (low)	°C	-	-	43.2	44.1	42.2	43.3	43.3
Absorber intermediate (middle)	°C	48.3	47.7	49.4	49.3	47.5	49.1	49.9
Absorber intermediate (middle)	°C	-	-	52.9	52.9	50.8	52.3	53.3
Absorber top of packing	°C	-	-	57.3	57.1	53.2	56.9	57.8
Water wash in	°C	44.8	45.2	46.1	47.5	44.9	48.2	48.4
Water wash outlet	°C	28.1	28.2	25.5	-	28.7	27.3	28.1
Cross HX-rich inlet	°C	32.7	31.8	32.3	34.8	31.1	33.6	31.6
Cross HX-rich outlet	°C	89.2	91.0	90.6	91.6	91.9	93.5	94.9
Cross HX-lean inlet	°C	102.0	102.0	103.0	103.0	103.0	104.0	105.0
Cross HX-lean outlet	°C	35.4	35.1	35.9	38.1	35.3	37.2	36.3
Reboiler	°C	120	120	120	120	120	120	120
<i>Pressure in stripper top</i>	barg	0.94	0.95	0.94	0.95	0.95	0.95	0.95
<i>Capture rate</i>								
Gas side (in-out of absorber)	%	62	58	67	55	71	55	68
Gas side (in-out of stripper)	%	60	56	42	42	-	-	61
Liquid side	%	-	-	82	81	79	63	88
<i>Emissions after abs. wash</i>								
1-(2HE)PRLD	mg/Nm ³	224.0	38.9	258.0	176.0	259.0	35.7	-
3A1P	mg/Nm ³	19.6	19.7	32.6	11.4	8.8	5.4	-
NH ₃	mg/Nm ³	1.3	1.7	3.6	8.1	5.9	4.3	-



The deviations observed in the gas phase side calculations are attributed mainly to uncertainties in the measurements of CO₂ concentration by FTIR on the top of the absorber wash and the gas flow measurements both in the absorber and the stripper side. Gas flow is measured in volumetric, positive displacement flow meters that have a rotating axle and are filled with water. This water level must be stable at a specific level for high accuracy measurement. During the measurement, water is condensing from the gas, therefore, changing the water level and increasing the measurement uncertainty. It is observed that the amount of water condensing in the measurement of the absorber gas flow can be considerable, thus, the operator empties the excess water in the flow meters before the measurement.

Uncertainties in pressure and temperature also propagate in the calculations through the conversion of volume to normal (Nm³) conditions. Following the calibration check of the FTIR measurements, as reported in Table 7, the accuracy of the gas flowmeters was also checked against reference values (Table 9). The reference values were controlled by an MFC, and the range was chosen to cover the design range of the flowmeters. It is seen that the measurements are relatively good, with larger deviations shown for the absorber flowmeter up to ARD=5.5% at flowrates of 1000 NL/h (deviation of 1 L/min) while the measurements conducted in the campaign are at the higher flowrates, for which lower deviations are observed. Even if the largest deviation is assumed, the differences are too small to explain the differences seen between the absorber-side and the stripper-side capture rate calculations.

Table 9. Comparison flowrate measurement with reference value.

Reference NL/h	Measurement L/h	Measurement NL/h	AD* NL/h	ARD** %
Absorber Flowmeter				
600	660	611	10.8	1.8
800	900	833	32.9	4.1
1000	1140	1055	55.0	5.5
1500	1620	1499	0.8	0.1
2000	2130	1971	28.8	1.4
3000	3240	2998	1.5	0.1
Stripper Flowmeter				
250	264	244	5.7	2.3
350	366	339	11.3	3.2
500	528	489	11.4	2.3
600	630	583	17.0	2.8

*Absolute Deviation. $AD = |CO_{2\text{ FTIR}} - CO_{2\text{ ref}}|$

**Absolute Relative Deviation. $ARD = |CO_{2\text{ FTIR}} - CO_{2\text{ ref}}| / CO_{2\text{ ref}}$

The capture rate when calculated based on the liquid analysis is consistently higher than the capture rate from the gas side. Such deviation is associated to the errors in measurements of liquid flow and, primarily, the liquid sample analysis. However, when taking into account the reported experimental error, it cannot adequately explain the deviations seen.



Moreover, the variations in CO₂ content in the studied stacks, from 5.6 to 8.2 vol%, does not indicate a direct effect on the capture rate. For the same solvent composition, and therefore same absorption capacity, an increase in capture rate is expected as the CO₂ concentration is reduced from ~8 to ~6%. However, due to the fact that the solvent was diluted (down to 31wt% amine, 1-(2HE)PRLD + 3A1P) as the campaigns progressed, no such observation can be made. Unfortunately, delays in the transportation of the samples led to limited information on the solvent composition in real time so as corrections could be applied.

As far as the emissions are concerned, high amine emissions up to ~250 mg/Nm³ are shown mainly in the start of each campaign with decreasing emissions along the campaign. These emissions are considered an important point of attention given the presence of one water wash and indicates the need for potentially two water washes. The measurement reported is after the miniplant reached stable conditions, therefore the high amine emissions seen in the start of the campaigns is not due to low solvent loading in start-up. The water wash temperature is also the same/very similar in the start and the end of the campaign, thus cannot explain this difference either. A study on the water wash removal efficiency with HS-3 and synthetic flue gas with ~5 vol% CO₂ was performed prior to the on-site campaign [3], and it was found to be ~ 90%. It is reminded that the position of the FTIR was fixed (explained in sub-section 4.1), therefore it was not possible to measure before and after the absorber on-site. The main contribution to emissions is from 1-(2HE)PRLD, as shown in *Figure 3*, and it is believed that this is due to its significantly higher volatility. Some extreme measurements which are recorded are expected to be outliers and do not coincide with any outstanding events during the campaigns. 3A1P and ammonia emissions were kept relatively low with average value less than 13 mg/Nm³ and 9 mg/Nm³, respectively.

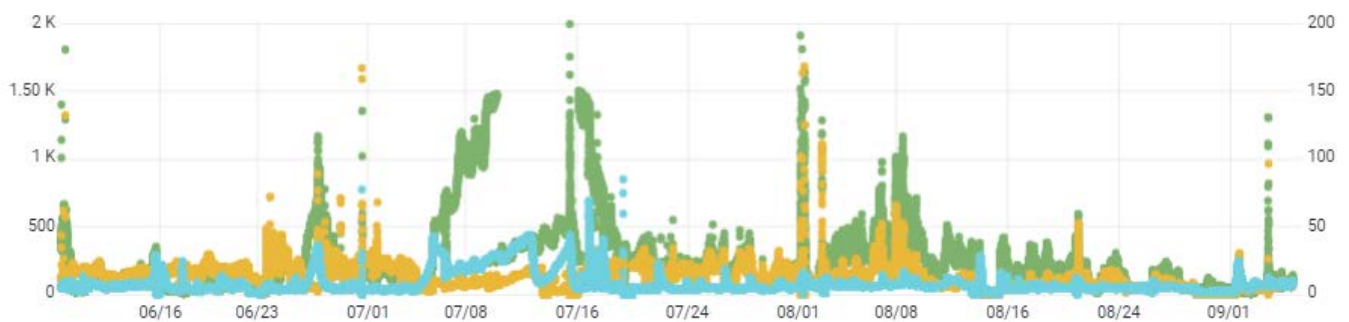


Figure 3. Amines and ammonia emissions in the course of the demonstration campaigns at Whitegate. 1-(2HE)PRLD: green, read in left y-axis; 3A1P: yellow, read in the right y-axis; ammonia: blue, read in right y-axis.

It is noted that high emissions could be also the result of aerosol-based emissions, which are more pronounced in the presence of particles and SO_x [4], [5] and which could not be confirmed in this work, as explained in sub-section 4.1. This could be the case especially in the instances where both amines and ammonia increase sharply, and quickly return to their previous lower levels.



4.3 Stability of HS-3 solvent

The results concerning the stability of the amine-constituents of HS-3, degradation products as well as metal concentrations are presented in this sub-section. The measurement of metals' concentration serves as an indicator of corrosion. It is noted that, prior to the demonstration activities in Irving Oil, the solvent has been used for the commissioning of the miniplant during preparation and de-risking activities in the laboratory. Therefore, the operating hours of the first samples of the demonstration start at 1019 operating hours.

4.3.1 Degradation trends

Samples were withdrawn and sent for analysis in the course of the campaign, with more than 3000 operating hours at stable conditions. It was found that the FTIR-ATR method is not suitable for analyzing liquid samples of HS-3 due to overlapping spectra of the main amines, therefore other type of more complex analysis such as LC-MS should be used. All lean samples were analysed for the solvent amines as well as total amine (alkalinity) by acid/base titration. The results are summarized in *Figure 4*, in which also the analysed results for total nitrogen in selected samples are included. There can be seen that there is good agreement for the trend between the total amine and the sum of the solvent amines determined by LC-MS. As can be seen the total amine are slightly higher than the sum of the two solvent amines by LC-MS, which is reasonable as there is also contribution from degradation products with amine functionality (like pyrrolidine) to the total amine. The total nitrogen is mainly equal or somewhat higher than the total amine. For the mol ratio of 3A1P over 3A1P+1-(2HE)PRLD, there is a decrease in the first part (until around 1353 hrs) and then fairly stable around 0.35 for the rest of the campaign as illustrated in *Figure 5*.

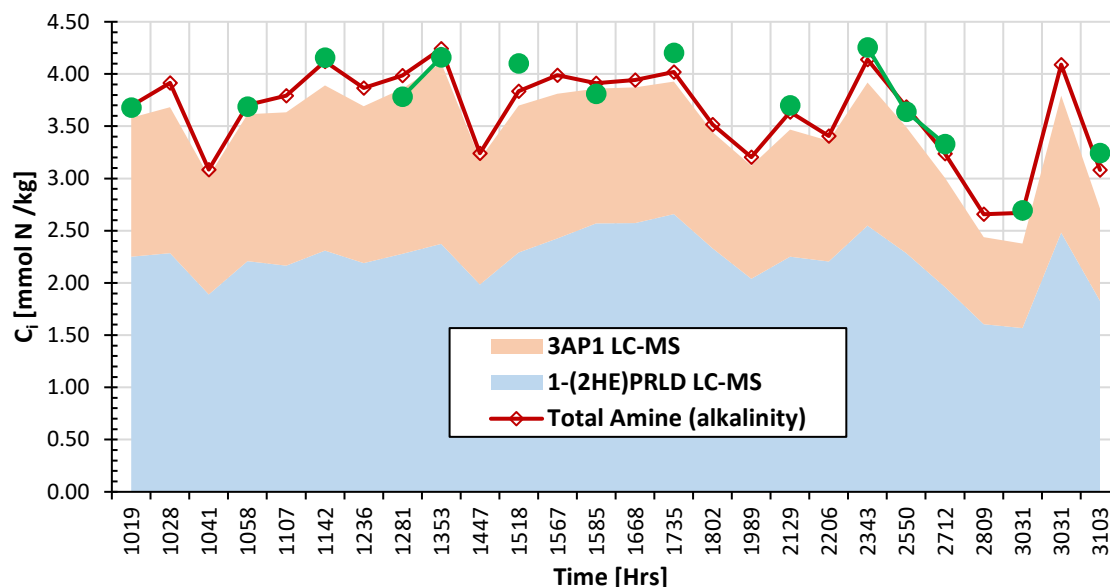


Figure 4. Comparison of total amine determined by acid/base titration, solvent amines by LC-MS and Total N determined by Shimadzu TOC-L CPH TNM-L (chemiluminescence detector).



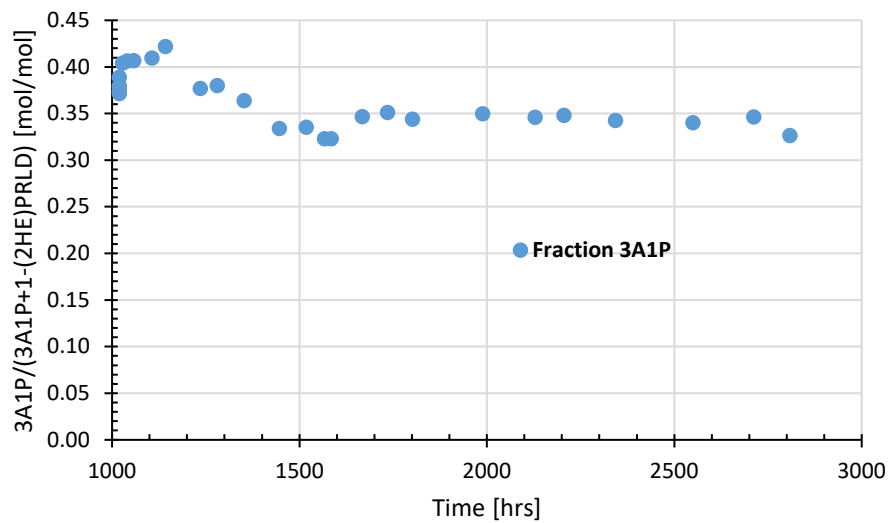


Figure 5. Molar fraction of 3A1P with respect to the sum of the two solvent amines in lean samples.

From the set of lean samples, there were selected samples for a range of degradation compounds (totally 41 degradation compounds were included in the analysis) which were analysed by LC-MS. These selected lean samples were also analysed for total nitrogen, metals by ICP-MS, and some of them also for total heat stable salts (HSS) by a wet chemistry method. The distribution of the major and minor degradation products is given in Figure 6. We can see that pyrrolidine, AP-urea, ammonia, HPGly and Methyl-AP are the major components, in agreement with the observations in the smaller lab-scale set-up where the solvent was tested before demonstration campaigns were started [6]. The sum of the determined nitrogen containing degradation compound in the last lean samples is around 2% relative to the start composition of 5 mol/kg.

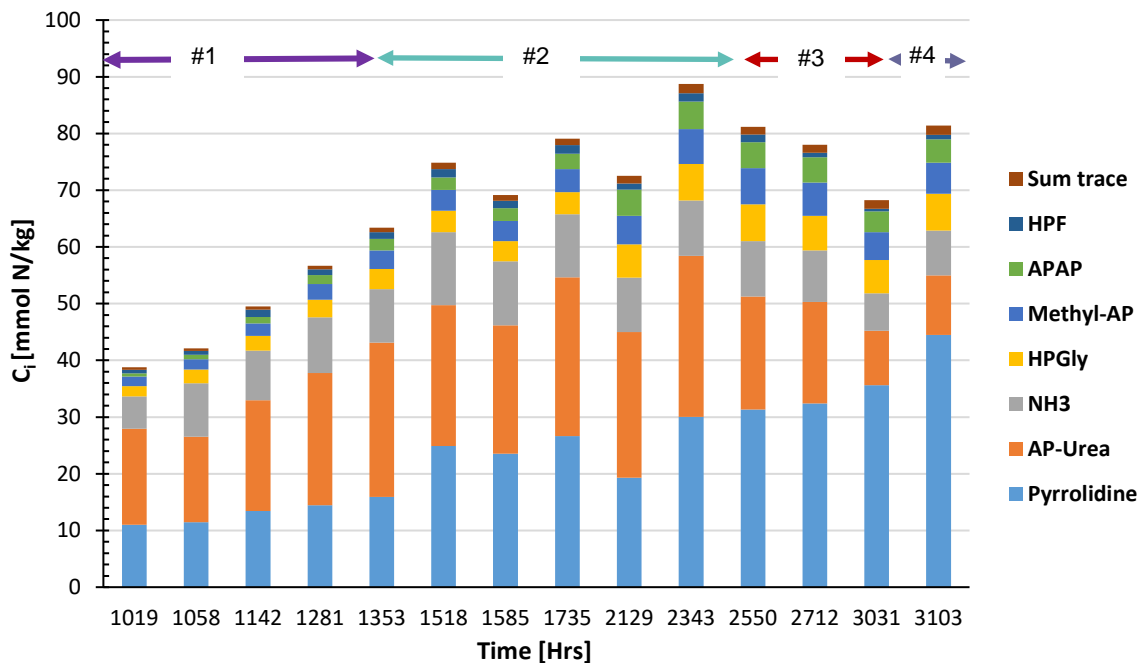


Figure 6. Distribution of major and minor degradation products (AP-urea, Pyrrolidine, HPGly, Methyl-AP, HPF, APAP, and NH₃) in lean HS-3 during the campaign.



To easier observe the development of the different degradation products, these are also plotted versus time in *Figure 7* (major & minor) and *Figure 8* (trace). For the major and minor compounds, it is seen that pyrrolidine has the largest increase (especially at the last part of the campaign). AP-Urea, however, has a different development, with a clear increase for the first part followed by a relatively stable level and then a significant decrease for the last part, else the major or minor have constant of slightly increasing trend.

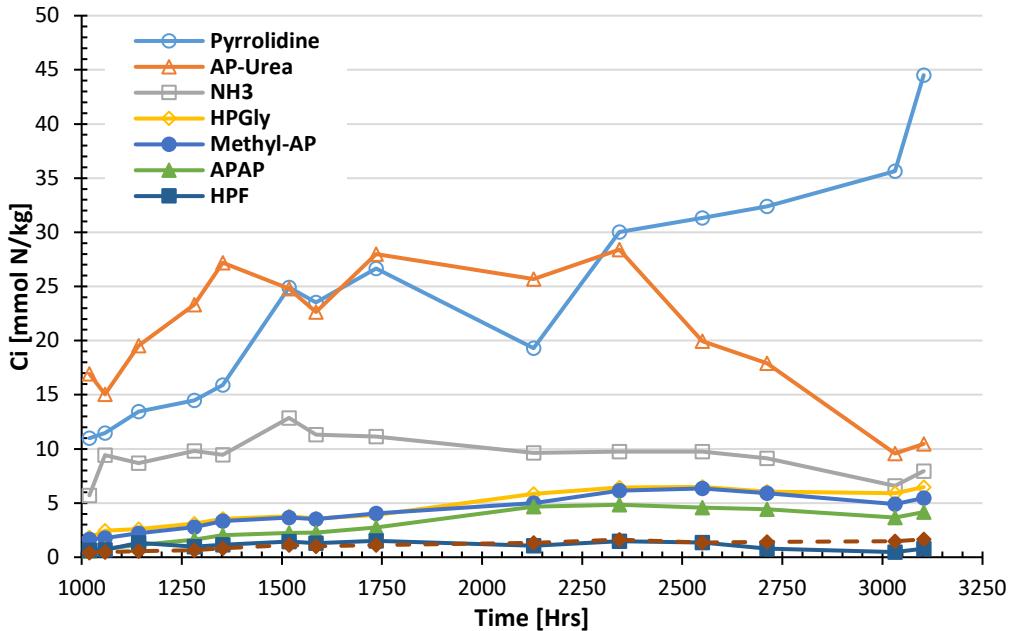


Figure 7. Development of major and minor degradation products (AP-urea, Pyrrolidine, HPGly, Methyl-AP, HPF, APAP, and NH3) in lean HS-3 during the campaign.

For the trace degradation compounds, HPAIa and tHHPP is the one which have the most increasing trends during the campaign. OZN have trend similar to AP-Urea.

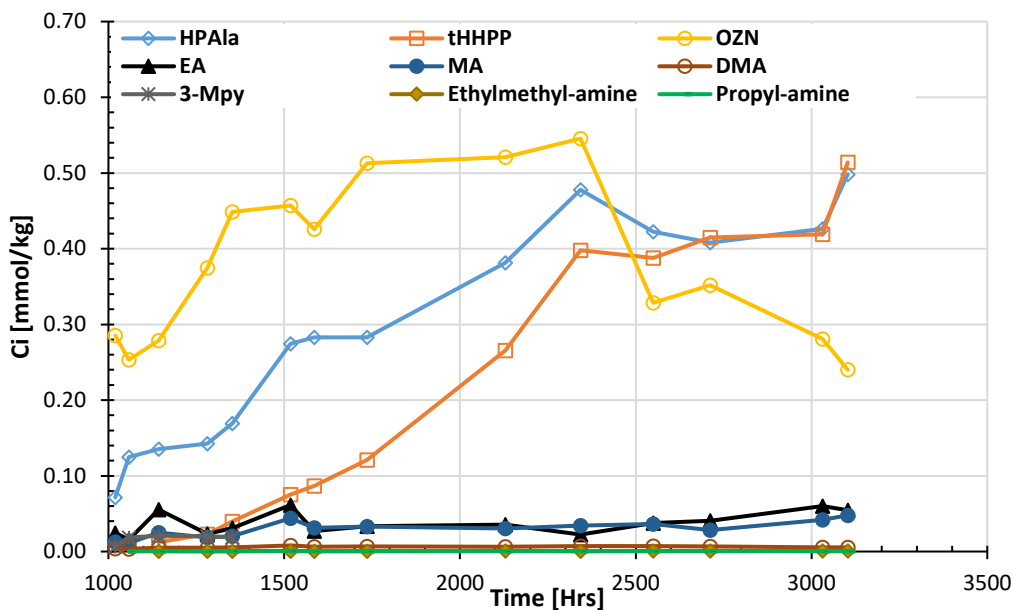


Figure 8. Development of trace degradation products (HPAIa, tHHPP, OZN, EA, MA, DMA, 3-Mpy, Ethylmethyl-amine and Propyl-amine) in lean HS-3 during the campaign.



The selected lean samples were also analyzed for a range of nitrosamines, however only two of them were above the Lower Limit of Quantification (LOQ). These were NPYR and Nitroso-N-Methyl-AP, which are the nitrosamines from the two degradation products pyrrolidine and N-Methyl-AP, respectively. The development of these two are shown in *Figure 9*, where a fairly constant increase can be observed for Nitroso-N-Methyl-AP, while NPYR shows a relatively large increase for the first part, followed by a decrease and then a relatively large increase for the last part.

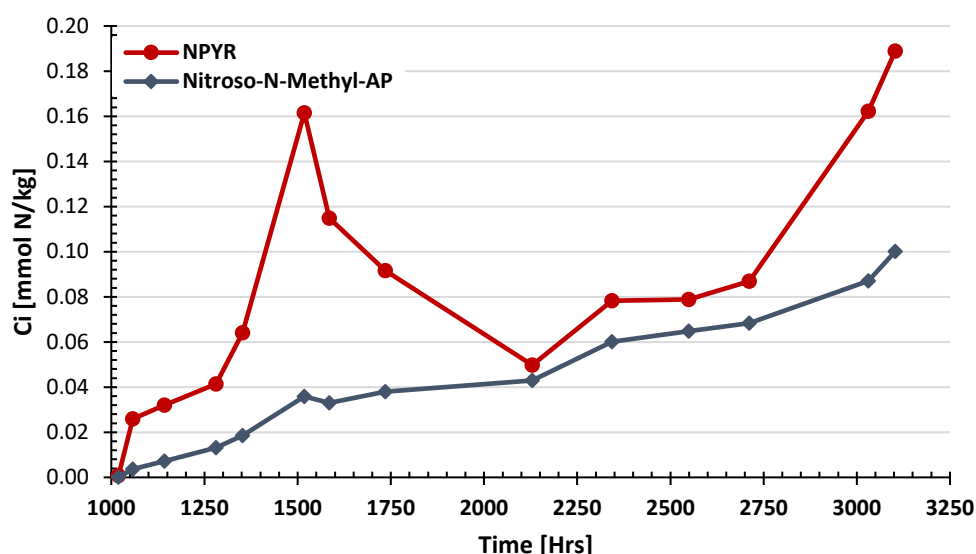


Figure 9. Concentration of NPYR and Nitroso-N-Methyl-AP in selected lean samples.

As mentioned earlier, the selected lean samples were also analyzed for total nitrogen, which is then used for check of the nitrogen balance in the samples. The nitrogen balance is the sum of nitrogen of all analyzed nitrogen containing compounds relative to the determined total nitrogen. The results of the nitrogen balances are summarized in *Figure 10*. Taking into account analytical uncertainties, the nitrogen balance is mainly closed. There may be some question for the last samples as in that case the nitrogen balance is just below 90%.

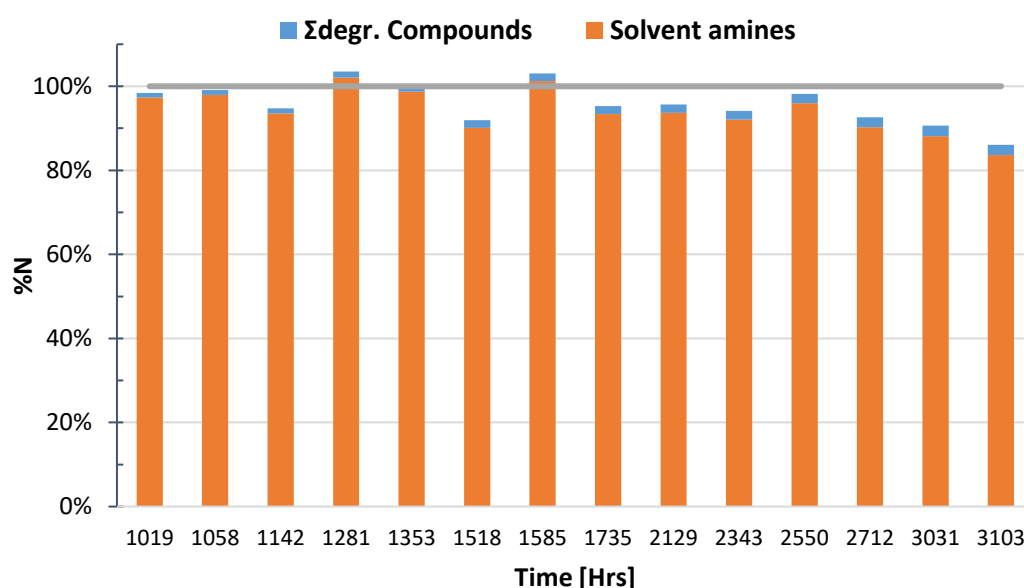


Figure 10. Nitrogen balance over the lean samples.



The selected lean samples were also analysed for 9 carboxylic acids (by LC-MS) which could be assigned as specific heat stable salts, as well as total heat stable salts (HSS). Amongst the carboxylic acids, formic, glycolic, lactic acid and acetic were observed above 25 mg/kg, with concentration of 224, 208, 98 and 74 mg/kg in the last lean sample respectively. For the determined total HSS, a fairly linear increase during the campaign could be observed, as depicted in *Figure 11*. Additionally, acetaldehyde, formaldehyde and acetone were analysed in the selected lean samples and the results were below 50 mg/kg for all of them.

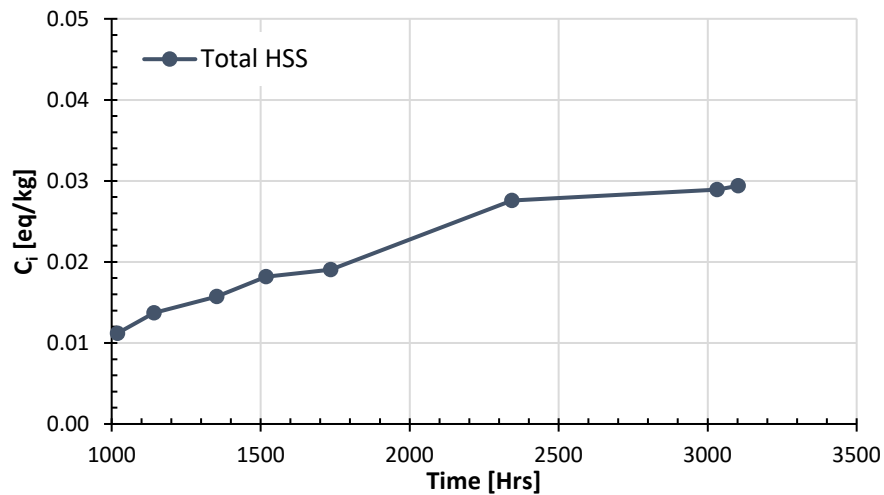


Figure 11. Total HSS (determined by wet chemistry method) in selected lean samples during the campaign.

4.3.2 Metals' concentration and corrosion

Metals, while at trace levels in the flue gas, are seen to be detectable in the miniplant solvent 25L inventory overtime. A selected number of miniplant solvent samples has been analysed for metal content from the real flue gas campaign using ICP-MS, specifically for Fe, Cr and Ni. The obtained data points are presented in *Figure 12*. The measured concentrations are below 2 mg/L for Fe and Cr and appears to be rather constant. For Ni there is an increase during the campaign, and the increase seems to be higher for the last part. In the last samples, the Ni concentration was 20 mg/L.

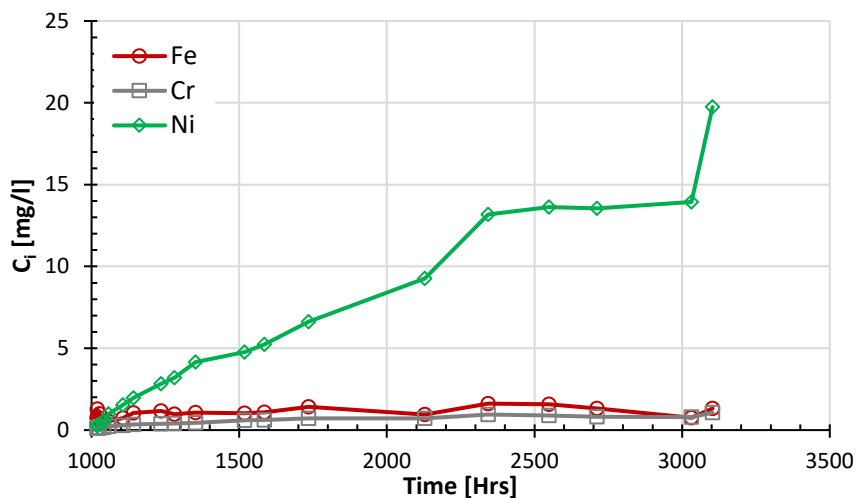


Figure 12. Metal content change in lean solvent during the test at Irving Oil .



5 Conclusions and further work

CO₂ capture using HS-3 solvent has been successfully demonstrated both in the laboratory with synthetic gas (TRL 5) and at Irving Oil Whitegate Refinery in Ireland with real flue gas (TRL 6). TNO's miniplant, an ATEX-compliant small-scale pilot plant, has been employed to capture CO₂ from the flue gas of four different sources of Irving Oil Whitegate Refinery. The results of these four campaigns, which lasted more than 3000 operating hours, give insights for the use of HS-3. The flue gases have varying content of CO₂, O₂ and other impurities in order to degrade and stress-test as much as possible the stability of the solvent. The operation with HS-3 showed that the solvent is easy to use, since it is non-toxic and did not precipitate, even during unplanned shut-downs. The solvent seems to show slow mass transfer, however it is noted that the solvent was diluted as the campaigns progressed. A point of attention is the high amine emissions with the use of one water wash, possibly attributed to the high volatility of one of its containing amines, 1-(2HE)PRLD. This points towards the requirement of using more than one water washes to control the emission levels.

In the analytical front, it was found that the FTIR-ATR method is not suitable for analyzing liquid samples of HS-3 due to overlapping spectra of the main amines, therefore other type of more complex analysis such as LC-MS should be used. The same degradation compounds were found in the campaigns with synthetic flue gas and real flue gases on-site, in agreement with what has been observed previously in a smaller cycled degradation rig, and the major components were AP-urea and pyrrolidine. With the exception of the last campaign, the nitrogen balance over the liquid samples was closed, indicating that the major degradation compounds with nitrogen have been accounted for. The results of the metal content analysis with synthetic and real flue gas, which was done to investigate any corrosion-related issues, show concentrations less than 2 mg/L of Fe and of Cr in the end of the campaign, though up to 20 mg/L for Ni.

The miniplant operation was performed in order to demonstrate the technology in a refinery and to degrade the solvent, after which the whole solvent inventory was sent to SINTEF's pilot plant in Tiller, Norway. By testing the solvent in this larger CO₂ capture plant, additional data and representative energy numbers will be obtained. In addition, 40 L of HS-3 solvent will be sent from SINTEF to TNO for demonstrating the countermeasures DORA and IRIS with synthetic flue gas at TNO's miniplant and for developing a reclaiming strategy for a two-amine solvent (one of which is volatile). This strategy will be developed by TNO, and a dedicated rig will be built for demonstrating the removal of impurities and 90% recovery of active solvent components.



6 References

- [1] A. Hartono *et al.*, “Characterization of 2-piperidineethanol and 1-(2-hydroxyethyl)pyrrolidine as strong bicarbonate forming solvents for CO₂ capture,” *Int. J. Greenh. Gas Control*, vol. 63, pp. 260–271, Aug. 2017, doi: 10.1016/J.IJGGC.2017.05.021.
- [2] A. Hartono, S. J. Vevelstad, I. Kim, R. Rennemo, and H. K. Knuutila, “Promoted Strong Bicarbonate Forming Solvents for CO₂ Capture,” *Energy Procedia*, vol. 114, pp. 1794–1802, Jul. 2017, doi: 10.1016/J.EGYPRO.2017.03.1307.
- [3] E. Skylogianni *et al.*, “Carbon Capture Demonstration at Irving Oil Whitegate Refinery,” *SSRN Electron. J.*, Nov. 2022, doi: 10.2139/SSRN.4277476.
- [4] P. Khakharia, J. Mertens, M. R. M. Abu-Zahra, T. J. H. Vlugt, and E. L. V. Goetheer, “Overview of aerosols in post-combustion CO₂ capture,” in *Absorption-Based Post-Combustion Capture of Carbon Dioxide*, Elsevier Inc., 2016, pp. 465–485.
- [5] J. G. M. S. Monteiro *et al.*, “Aerosol Emission at a Post Combustion CO₂ Capture Plant at Twence (WtE Facility),” in *TCCS-11 Proceedings*, 2021.
- [6] S. J. Vevelstad *et al.*, “Chemical stability and characterization of degradation products of blends of 1-(2-hydroxyethyl)pyrrolidine and 3-amino-1-propanol,” *Submitt. to Ind. Eng. Chem. Res.*, 2022.

